Eur. Phys. J. B **52**, 453–457 (2006)
DOI: 10.1140/epjb/e2006-00335-2

THE EUROPEAN PHYSICAL JOURNAL B

Poole-Frenkel conduction in Al/ZrO_2/SiO_2/Si structures

P.V. Aleskandrova[a], V.K. Gueorguiev, Tz.E. Ivanov, and J.B. Koprinarova

Institute of Solid State Physics, Bulgarian Academy of Sciences, 72 Tzarigradsko chausse Blvd., 1784 Sofia, Bulgaria

Received 3 May 2006
Published online 21 August 2006 –

Abstract. Leakage currents through Al/ZrO_2/SiO_2/n-Si metal-insulator-semiconductor (MIS) capacitors were studied. Thin SiO_2 films were chemically grown on monocrystalline phosphorous doped silicon wafers. Zirconia films with thicknesses of 15 and 50 nm were deposited by radio frequency (rf) magnetron sputtering and, then, annealed in oxygen ambient at 850 °C, for 1 h. The dielectric constant of the sputtered and annealed ZrO_2 layer was of about 17.8. The equivalent oxide thickness (EOT) of the stack 15 nm and 50 nm-ZrO_2/SiO_2 structure was estimated to be 3.2 nm and 10.7 nm, respectively. The temperature dependence of the leakage currents was explained by Poole-Frenkel (PF) conduction mechanism. Shallow trap levels in the studied structure of about 0.2 eV and 0.46 eV were calculated. The existence of A and D-defects, due to the sputtering and high temperature annealing in oxygen, was suggested.

PACS. 72.20.-i Conductivity phenomena in semiconductors and insulators – 73.40.Qv Metal-insulator-semiconductor structures (including semiconductor-to-insulator)

1 Introduction

Gate dielectric stacks of high-k materials have been proposed to enable the reduction of effective gate oxide thickness of MOSFETs (metal-oxide-semiconductor field effect transistors) below 2 nm which is necessary to allow further device scaling. Several high-k materials as alternative gate dielectrics – Si_3N_4, Al_2O_3, Ta_2O_5, HfO_2, ZrO_2 and etc., have been discussed in the literature [1–5]. Among the various high-k dielectrics, ZrO_2 has received a great attention due to its high dielectric constant (15–24), large band gap (5–7 eV) and high breakdown field (15–20 MV/cm) [6–8].

The quality of sputtered ZrO_2 films strongly depends on the deposition conditions – target power, gas pressure, deposition temperature, target composition, contaminations, thermal treatments, annealing, etc. The degree of crystallinity, interface roughness, chemical homogeneity, charge trapping phenomena and stoichiometry has a direct effect on the dielectric properties and the leakage currents across the dielectric layers. Post-deposition treatments also affect the electric and dielectric properties of zirconia [6,9]. High temperature treatments lead to formation of SiOx and/or Zr-silicate interfacial layers between the zirconia film and the silicon substrate [10]. Moreover, during the high temperature annealing in oxygen ambient, the thickness of the interfacial (SiOx or Si-O-Zr) layers could be increased, because of possible oxygen diffusion through ZrO_2 [11].

For the low-temperature monoclinic phase (<1200 °C) of ZrO_2 it was proven that there is a strong dynamic charge transfer along Zr-O bond as the bond length varies, indicating a mixed ionic-covalent nature of the Zr-O bond. Such an anomaly reflects on the relatively delocalized structure of the electronic charge distributions. It is quite common effect in other weakly ionic oxides such as ferroelectric perovskites [12].

Apart from the thermodynamic stability, interface quality and reliability, the dielectric permittivity and the barrier height are of essential importance as they influence the gate oxide leakage currents. The leakage current is a critical property for the quality and reliability of MOSFETs. Electrical characteristics of ZrO_2 and Zr-silicate thin layers, demonstrating low leakage currents have been reported in many papers [6,13].

Several types of conduction mechanisms including Poole-Frenkel emission, space-charge limited current (SCLC) and Schottky barrier limited conduction in ZrO_2 have been discussed in the literature [6,10,14,15]. Leakage currents through RTCVD (rapid thermal chemical vapor deposition), microwave PECVD (plasma enhanced chemical vapor deposition) and rf sputter deposited thin ZrO_2 layers, including the effect of image-force barrier lowering, have been studied. The tunneling currents have been modeled by Schottky barrier limited and Poole-Frenkel bulk limited emission. In these papers, the conduction mechanism through zirconia layer was interpreted as two field-dependent leakage current components – Schottky emission at low fields and Poole-Frenkel emission at high electric fields [6,10]. Through MOCVD (metal-organic chemical vapor deposition) deposited ZrO_2 thin films,

[a] e-mail: val@issp.bas.bg

a strong trap-assisted tunneling conduction, due to high trap concentration, was identified [15].

This paper reports about the results obtained on the voltage and temperature dependence of the leakage currents in $Al/ZrO_2/SiO_2/n$-Si metal-insulator-semiconductor (MIS) structures. The zirconia films were deposited by rf sputtering and annealed in oxygen-ambient at temperature of 850 °C, for 1 h. The electron tunneling through the stack structure complies with the Poole-Frenkel conduction mechanism.

2 Experiment

ZrO_2 capacitors were fabricated on n-type (100) silicon wafers with donor doping of about 1×10^{15} cm^{-3}. Chemical SiO_2 layer was grown on the silicon wafers in H_2SO_4:H_2O_2 (3:1) mixture for 20 min at temperature of 40 °C. Zirconia thin films with thicknesses 15 nm and 50 nm were deposited by rf magnetron sputtering from Zr target (LeskerCo. with purity 99.7%). The sputter gas was Ar/O_2 (90/10) mixture at a pressure 0.5×10^{-2} mbar. The samples were annealed at 850 °C in dry oxygen for 1 h. Top Al contacts were thermally evaporated and capacitors with area of 10^{-4} cm^2 were obtained. Finally, the samples were annealed at 425 °C for 30 min in a forming gas.

The $Al/ZrO_2/SiO_2/n$-Si capacitors were electrically characterized using a Keithley 617 programmable electrometer to obtain current-voltage $(I-V)$ curves. Capacitance-voltage $(C-V)$ measurements were performed by PAR 410 CV Plotter.

3 Experimental results and discussion

High frequency (1 MHz) $C-V$ measurements on the $Al/ZrO_2/SiO_2/n$-Si structures were performed. The dielectric permittivity of zirconia films of 17.8 was calculated. For the both thicknesses of ZrO_2 – 15 nm and 50 nm, the equivalent oxide thickness (EOT) of 3.2 nm and 10.7 nm was obtained, respectively.

The leakage currents at different temperatures and polarities of the applied voltage were performed. The leakage currents were measured at voltages applied from 0 V to +10 V and to −10 V with voltage step of 0.1 V, and time delay of 1 s.

Direct tunneling conduction through the thin SiO_2 film is suggested because of the small thickness of the layer. Thus, this conduction mechanism plays an unimportant role in the net conduction through the stack structure.

Two field-dependent leakage current components are distinguished from the leakage characteristics. At low electric fields, the density of traps, trap levels in the forbidden gap, oxide thickness and mobility of carriers determines the leakage currents. The electrical conduction and leakage currents at low electric fields will be examined in a future paper.

The high field region complies with either Poole-Frenkel or Schottky conduction mechanisms. At high fields two dominant mechanisms lead to rapid increase of the leakage current density – Schottky and Poole-Frenkel conduction. Schottky conduction is an electrode-limited emission and Poole-Frenkel conduction is a bulk-limited emission. In the both cases, the barrier height is decreased as a result of the applied field.

At Schottky conduction, carrier emission from the metal electrode into the conduction band of insulator, due to the barrier lowering, is observed. The energy of free carriers in the metal electrode and in the conduction band is equilibrated, and the Schottky barrier results from the created image forces.

In the case of Poole-Frenkel (PF) emission, the conduction is realized through charged traps in the bulk of insulator. The PF conduction mechanism dominates in insulators with high trap concentration [16]. Electron emission from the Coulombic donor-like centers is observed. Coulombic interaction between the emitted carriers (electrons) and the charged states (positively charged ions) appears. This field-dependent emission of carriers from the trap levels in the forbidden gap is used in order to be determined the charge state of the traps. The concentration and sign of the defects ionized after the emission could be determined. The sign of the ionized defects is opposite to that of the emitted carriers.

Usually, in any given insulator, the both conduction mechanisms are presented. The important issue is to be defined the dominated mechanism. The both conduction mechanisms show a current exponential function versus square root of the applied voltage which is described by the following equations:

$$J = A^* T^2 \exp\{\beta_{Sc} V^{1/2}\} \exp\{-q\Phi_B/k_B T\} \quad (1)$$

for Schottky effect and

$$J = (CV/L) \exp\{\beta_{PF} V^{1/2}\} \exp\{-q\Phi_T/k_B T\} \quad (2)$$

for Poole-Frenkel effect,
where J is the current density, V is the applied voltage, A^* is the effective Richardson constant, Φ_B is the Schottky barrier height, Φ_T is the ionization energy of the trap levels, k_B is the boltzman constant, T is the temperature, C is a constant related to the density of ionized traps and carrier mobility. β_{Sc} and β_{PF} are barrier lowering coefficients for the Schottky and Poole-Frenkel emission, respectively. Usually, β_{PF} is two times higher than β_{Sc}. The coefficients β_{Sc} and β_{PF} depend on the dielectric constant and the inter-electrode distance L according to

$$2\beta_{Sc} = \beta_{PF} = (q/k_B T)(q/\pi\varepsilon_0\varepsilon_{ox} L)^{1/2} \quad (3)$$

where ε_0 is the dielectric permittivity in vacuum, ε_{ox} is the static dielectric constant.

The calculated values of β_{Sc} and β_{PF} are: $\beta_{Sc} = 3.86$ eV cm$^{1/2}/V^{1/2}$ and $\beta_{PF} = 7.72$ eV cm$^{1/2}/V^{1/2}$ for 15 nm thick ZrO_2 film; $\beta_{Sc} = 1.56$ eV cm$^{1/2}/V^{1/2}$ and $\beta_{PF} = 3.11$ eV cm$^{1/2}/V^{1/2}$ for 50 nm thick ZrO_2 film. The experimental values, determined from $\ln(J/V)$ versus $V^{1/2}$ plots, are closer to the calculated β_{PF} values. Therefore, the dominant conduction mechanism in the studied

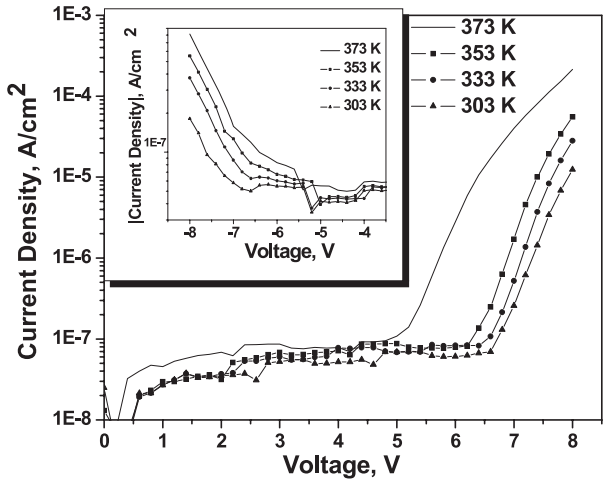

Fig. 1. Leakage currents measured on Al/15 nm ZrO_2/SiO_2/n-Si structure vs. temperature.

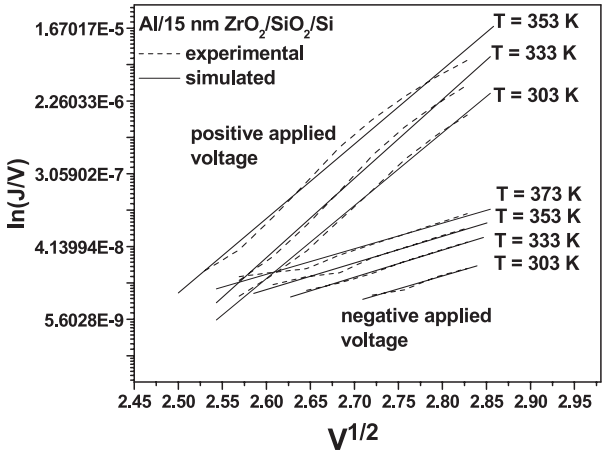

Fig. 2. Poole-Frenkel plot – $\ln(J/V)$ vs. $V^{1/2}$.

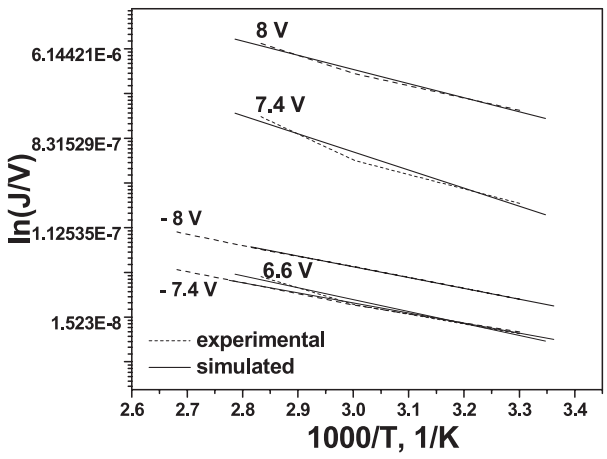

Fig. 3. Poole-Frenkel plot – $\ln(J/V)$ vs. $1/T$.

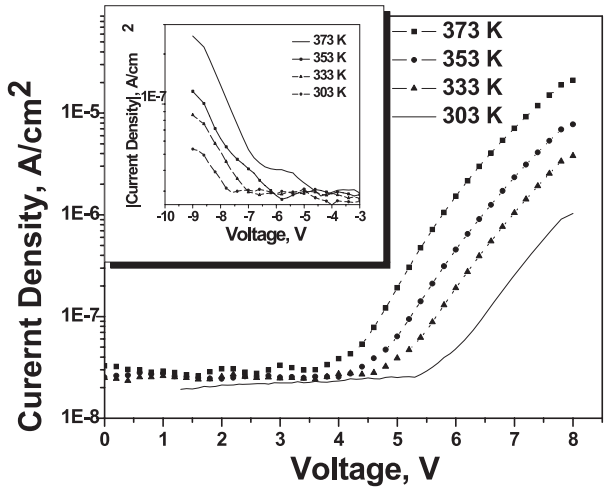

Fig. 4. Leakage currents measured on Al/50 nm ZrO_2/SiO_2/n-Si structure vs. temperature.

structure is the Poole-Frenkel emission. This result implies the presence of high density of structural defects in the bulk of insulator. Thus, the trap levels, due to the structural defects, will determine the conduction mechanism [17].

The temperature dependence of the leakage currents through 15 nm thick ZrO_2 film, at negative and positive bias, is presented in Figure 1.

The following method is used to extract the values of Φ_T and β_{PF}: (i) β_{PF} is defined from the slope of $\ln(J/V)$ versus $V^{1/2}$ plot; (ii) then, the value of β_{itPF} is taken with the slope of $\ln(J/V)$ versus $1/T$ curve in order to extract Φ_T value. The measured leakage characteristics at 303 K, 333 K, 353 K and 373 K coincide very well with the exponential trace of curves.

In case of 15 nm thick ZrO_2 film, at positive and applied voltages, the PF $\ln(J/V)$ versus $V^{1/2}$ plot is shown in Figure 2. The leakage current density plotted as a function of temperature at a constant voltage is presented in Figure 3. The slope of the $\ln(J/V)$ versus $V^{1/2}$ plot coincides with the slope of the measured $I-V$ characteristics at positive and negative voltages. At positive applied voltages, the β_{PF} coefficient and energy of trap level Φ_T of about 20.83 eV $\mathrm{cm}^{1/2}/V^{1/2}$ and 0.28 eV is extracted, respectively. In the case of negative applied voltages, the β_{PF} coefficient is about 7.22 eV $\mathrm{cm}^{1/2}/V^{1/2}$ and the trap level Φ_T is about 0.22 eV.

The temperature dependence of leakage currents, through 50 nm thick ZrO_2 film at negative and positive voltage ramps, is presented in Figure 4. The current-voltage characteristics were measured at the following temperatures 303 K, 333 K, 353 K and 373 K.

The calculated barrier lowering coefficient and trap level value, in case of negative voltage ramps, is about 3.02 eV $\mathrm{cm}^{1/2}/V^{1/2}$ and 0.18 eV, respectively. At positive voltage ramps, the following values are extracted $\beta_{PF} =$ 7.65 eV $\mathrm{cm}^{1/2}/V^{1/2}$ and $\Phi_T = 0.46$ eV. The experimental $\ln(J/V)$ versus $V^{1/2}$ and $\ln(J/V)$ versus $1/T$ plots are shown in Figures 5 and 6, respectively.

In cases of positive and negative voltage polarities, the voltage values, at which the leakage current suddenly increases, are different. When negative voltage is applied on the metal electrode, the metal represents the cathode and the carriers are injected into ZrO_2. Under positive voltage,

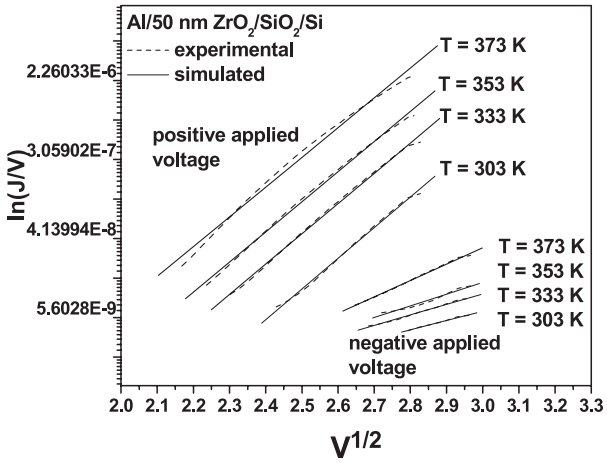

Fig. 5. Poole-Frenkel plot – $\ln(J/V)$ vs. $V^{1/2}$.

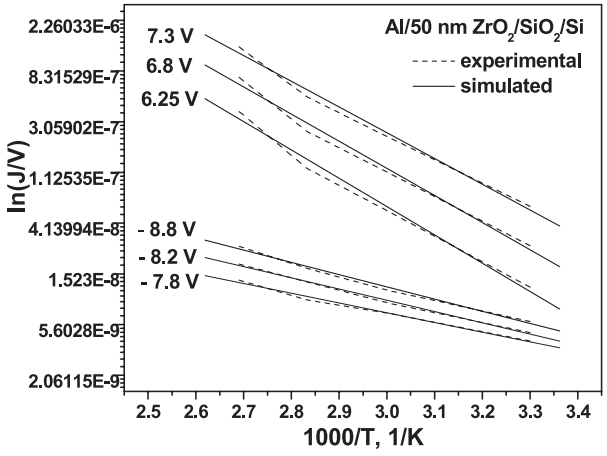

Fig. 6. Poole-Frenkel plot – $\ln(J/V)$ vs. $1/T$.

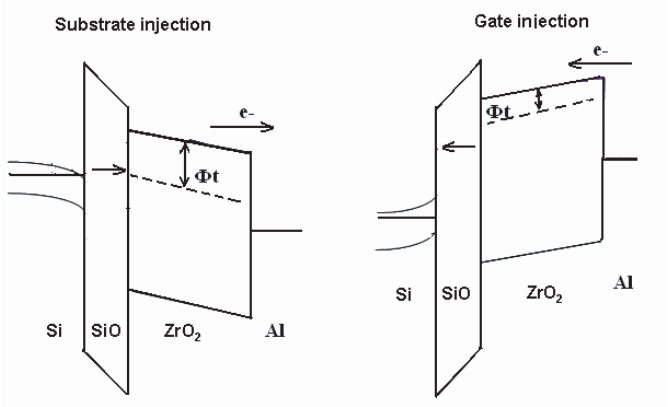

Fig. 7. Energy band diagrams at substrate and gate injection.

the silicon substrate injects electrons into the insulator. The energy band diagrams of the structure, at positive and negative applied voltage, are given in Figure 7.

The obtained results show that, at positive voltages, the experimental β_{PF} value is about 2.5 times higher than the β_{PF} value at negative voltages. This corresponds to the sharply increase of the leakage current at positive voltages in comparison to the leakage characteristic at negative voltages. Houssa have reported [18] that the probability for electron tunneling under substrate injection is larger than that at gate injection. It is due to the asymmetry of the energy band diagram of the MIS structure (Fig. 15).

The extracted ionization energy level at substrate injection is higher than the calculated energy level at gate injection. In case of substrate injection, trap energy levels of about 0.28 eV and 0.46 eV were calculated. In case of gate injection, trap energy levels of about 0.22 eV and 0.18 eV were extracted.

In some papers about the PF emission through ZrO_2 thin films, trap levels in range of 0.78–0.86 eV have been published [14,19], but in these papers, the ZrO_2 layers were obtained by PECVD and UHV-ozone oxidation techniques. The trap level of 0.8 eV below the conduction band corresponds to D-defects. The D-defect is the first ionization level of the oxygen vacancy deep double donor [20,21]. Probably, the deeper level of 0.46 eV corresponds to D-defects.

The calculated trap level of 0.2 eV could be related with A-defects [21]. The A-defect is a donor level with energy of about 0.2 eV below the conduction band. The A-defects show up in metal-oxide insulators on Si after high temperature annealing. The defects are related to the oxygen vacancies and Si contaminations, and represent Si/O-vacancy complex single donor. Obviously, the origin of the trap level is due to the presence of oxygen defects and interstitials at the ZrO_2/SiO_2 and SiO_2/Si interfaces. Similar defect levels have been found in Ta_2O_5 thin layers, deposited by LP-MOCVD technique [21]. Moreover, it has been reported for HfO_2 [22], TiO_2 [23], SnO_2 [24] that oxygen vacancies induce electronic states in the band gap. The influence of oxygen vacancies seems to be general for metal oxides.

During high temperature treatments, most of the single acceptors are ionized and become negatively charged, and most of the deep oxygen vacancy double donors are ionized, and become positively charged. Moreover, at high temperatures, atoms can move relatively easily, especially in ionic insulator, where, the movement is not strongly restricted by rigid covalent bonds. Thus, the charged states related to the oxygen vacancies and the negatively charged oxygen atoms, located near to the ZrO_2/SiO_2 and SiO_2/Si interfaces, will be increased.

An important issue of the quality of zirconia depends on the oxygen stoihiometry and formation of oxygen defects. The defects formed by an interstitial oxygen atom can form three different charge states – neutral oxygen interstitials, positively charged oxygen interstitials and negatively charged oxygen interstitials [25]. For instance, when an electron is added to a neutral oxygen interstitial, the interstitial undergoes large displacement forming a negatively charged interstitial. Additionally, in ZrO_2 thin films there are three type oxygen vacancies – neutral

vacancy, positively charged vacancy and negatively charged vacancy. Ionization of the neutral vacancies results in the creation of positively charged defects. Trapping of an additional electron at a neutral vacancy leads to creation of a negatively charged vacancy. These defects are important at the interface with silicon and may serve as an electron source. The oxygen interstitials and vacancies can capture electrons from the conduction band of the metal and/or silicon.

Finally, it must be noted that there is no clear distinction between the bulk limited and electrode limited conduction processes, because each plays a part in the conduction mechanism. For example, the density of free carriers is electrode limited, while the mobility, which determines the velocity, is a bulk limited property etc. In this study, the bulk limited conduction (Poole-Frenkel emission) through sputtered and annealed at high temperature in oxygen ambient zirconia thin layers was observed.

4 Conclusion

The electrical properties of the $Al/ZrO_2/SiO_2/n$-Si structures at different temperatures and voltage polarities were studied. The dominant conduction mechanism in the studied structures is Poole-Frenkel emission. This result determines the presence of high density of structural defects in the bulk of insulator.

On the base on the experimental data and the theoretical background, it could be concluded:

(i) During the positive voltage scan, the electron tunneling is determined by deeper trap levels about 0.46 eV.
(ii) During the negative voltage scan, the conduction is realized through trap levels about 0.20 eV.
(iii) The extracted trap levels could be related with A and D-defects representing Si/O-vacancy complex single donor and the first ionization level of oxygen vacancy deep double donor. The presence of such defects is due to the deposition conditions and the high temperature oxygen annealing.

Financial support from the Swiss National Science Foundation – Project No. IB7420-110981/1 "Southern NanoEngineering Network" (SONNET) is highly appreciated by the authors.

References

1. D.A. Buchanan, IBM J. Res. Develop. **43,** 245 (1999)
2. Hon-Sum P. Wong, D.J. Frank, P.M. Solomon, C.H.J. Wann, J.J. Welser, Proc. IEEE **87**, 537 (1999)
3. N. Yang, W.K. Henson, J.J. Wortman, Tech. Dig.- Int. Electron Devices Meet., 453 (1999)
4. S.H. Lo, D.A. Buchanan, Y. Taur, W. Wang, IEEE Electron Device Lett. **18**, 209 (1997)
5. J.H. Stathis, D.J. DiMaria, Tech. Dig.- Int. Electron Devices Meet., 167 (1998)
6. Fu-Chien Chiu, Zhi-Hong Lin, Che-Wei Chang, Chen-Chih Wang, Kun-Fu Chuang, Chih-Yao Huang, Joseph Ya-min Lee, Huey-Liang Hwang, J. Appl. Phys. **97**, 0345061 (2005)
7. M. Balog, M. Schieber, M. Michman, S. Patai, Thin Solid Films **47,** 109 (1977)
8. B. Kralik, E.K. Chang, S.G. Louie, Phys. Rev. B **57**, 7027 (1998)
9. M. Bhaskaran, P.K. Swain, D. Misra, Electrochem. Solid-State Lett. **7**, F38 (2004)
10. J.P. Chang, Y.S. Lin, Appl. Phys. Lett. **79**, 3666 (2001)
11. J.M. Howard, V. Cracium, C. Essary, R.K. Singh, Appl. Phys. Lett. **81**, 3431 (2002)
12. X. Zhao, D. Vanderbilt, Phys. Rev. B **65**, 0751051 (2002)
13. G.D. Wilk, B. Brar, IEEE Electron Device Lett. **20**, 132 (1999)
14. S. Ramanatham, Chang-Man Park, Pol McIntyre, J. Appl. Phys. **91**, 4521 (2002)
15. A. Gehring, S. Harasek, E. Bertagnolli, S. Selberherr, IMEC Report (2003)
16. S.D. Ganichev, E. Ziemann, W. Prettl, I.N. Yassievich, A.A. Istrarov, E.R. Weber, Phys. Rev. B **61**, 10361 (2000)
17. J. Frenkel, Phys. Rev. **54,** 647 (1938)
18. M. Houssa, IMEC-Report (2001)
19. S. Chakraborty, M.K. Bera, G.K. Dalapati, D. Paramanik, S. Varma, P.K. Bose, S. Bhattacharya, C.K. Maiti, Semicond. Sci. Technol. **21**, 467 (2006)
20. H. Sawada, K. Kawakami, J. Appl. Phys. **86**, 956 (1999)
21. W.S. Lau, L.L. Leong, T. Han, N.P. Sandler, Appl. Phys. Lett. **83**, 2835 (2003)
22. H. Takuechi, D. Ha, T.-J. King, J. Vac. Technol. A **22,** 1337 (2004)
23. S. Munnix, M. Schmeits, Phys. Rev. B **31**, 3369 (1985)
24. J.M. Themlin, R. Sporken, J. Darville, R. Caudano, J.M. Gilles, R.L. Johnson, Phys. Rev. B **42,** 11914 (1990)
25. A.S. Foster, V.B. Sulimov, F. Lopez Gejo, A.L. Shluger, R.M. Nieminen, Phys. Rev. B **64**, 2241081 (2001)